DOI: 10.23968/2500-0055-2023-8-1-82-87

STUDYING THE OPERATION OF THE PNEUMOHYDRAULIC SHOCK ABSORBER WITH ZERO BOTTOMING IN THE SUSPENSION OF A TRANSPORT AND HANDLING MACHINE

Sergey Repin*, Ivan Vorontsov, Denis Orlov, Roman Litvin

Saint Petersburg State University of Architecture and Civil Engineering
Saint Petersburg, Russia

*Corresponding author's e-mail: repinserge@mail.ru

Abstract
Introduction: The movement smoothness of transport and handling machines (THM) (excavators, cranes, road maintenance equipment, etc.) on a vehicle chassis significantly affects their durability as a result of the large weight of equipment and uneven load distribution along the axes of the base chassis, which causes heavy dynamic loads when moving along roads with imperfect pavement. However, THM often have to move along those very roads. **Purpose of the study:** We aimed to increase the movement smoothness of THM on a vehicle chassis by using a shock absorber of new design as the main vehicle undercarriage suspension element. **Methods:** The hydropneumatic shock absorber is considered the most common. The principle of its operation is based on hydraulic resistance that occurs when the piston with the rod move in a space filled with oil, while the gas in the closed part is compacted, compensating for changes in the internal volume. Most often, the main disadvantage related to the operation of hydropneumatic shock absorbers (HPSA) is the probability of bottoming when hitting a barrier (obstacle), which results in dynamic loads reducing the service life of the vehicle and the parts of the shock absorber. **Results:** The paper describes a new shock absorber design ruling out bottoming, provides a mathematical model of its elastic response, and presents the results of modeling in Mathcad, confirming the operability of the device.

Keywords: movement smoothness, shock absorber, elastic response.

Introduction

The movement smoothness of transport and handling machines (THM) (excavators, cranes, road maintenance equipment, etc.) on a vehicle chassis significantly affects their durability as a result of the large weight of equipment and uneven load distribution along the axes of the base chassis, which causes heavy dynamic loads when moving along roads with imperfect pavement. However, THM often have to move along those very roads. Particularly heavy dynamic loads occur when they move over large irregularities causing shock absorber bottoming. Often, after relocation, it may be required to repair mechanical damage to the operating equipment.

The movement smoothness of THM is guaranteed by a system of devices ensuring elastic connection between the wheels and the body, called suspension. The suspension absorbs energy from bumps and shocks that occur while moving along the road. The suspension includes both damping and elastic components. The latter reduce the dynamic load that occurs during suspension operation when moving over rough roads. The elements of the damping components dampen the vibrations of the body. In standard suspensions, damping and elastic components are usually separated and operate in parallel (Carway.info, 2017), Dobromirov et al., 2006; Rotenberg, 1972).

The hydropneumatic shock absorber is considered the most common. The principle of its operation is based on hydraulic resistance that occurs when the piston with the rod move in a space filled with oil, while the gas in the closed part is compacted, compensating for changes in the internal volume. Most often, the main disadvantage related to the operation of hydropneumatic shock absorbers (HPSA) is the probability of bottoming when hitting a barrier (obstacle), which results in dynamic loads reducing the service life of the vehicle and the parts of the shock absorber.

Recently, an elastic component has been introduced into this type of suspension, which makes it possible to change the stiffness and clearance of the suspension. The operation of this component is based on a pneumatic cylinder (Akopyan, 1979; Chelomey, V. N.,1981; Lukin, P. P. et al., 1984; Techautoport.ru, 2022). This scheme significantly reduces the probability of shock absorber operation in bottoming when it is compressed. Besides, it has a complex design because its parts are made in the

form of individual components. These components require other attachment points for full operation, as well as space for placement and connection with the linkage system.

Widely distributed HPSA meet the requirements for the functionality of suspensions: the combination of a hydro cylinder and a pneumatic cylinder makes it possible to achieve the effect of a “gas spring” (Audi, 2001; Zaitsev, A. V.,2007; Zhileykin, M. M. et al., 2012; Repin et al., 2019; Repin et al., 2020). The specifics of their operation is in reducing the risk of HPSA bottoming during compression, but at rebound the probability of bottoming remains quite high. Thus, as a result of studies and HPSA modeling, a new scheme of HPSA operation with two hydraulic and pneumatic cylinders installed both above and below was proposed, which significantly reduced the probability of HPSA bottoming both during compression and rebound.

During the studies, we simulated the operation of the modified HPSA equipped with two gas springs placed above and below the hydraulic part of the shock absorber and ruling out its bottoming during compression and rebound.

Shock absorber operation

Fig. 1 presents a new shock absorber design (Repin, 2022).

Places of rigid connection are shown with crosses.

Chambers G1 and G3 act as an elastic element (gas springs) and rule out shock absorber bottoming during compression (G1) and rebound (G3). The clearance can be adjusted on account of the difference in the values of pumping pressure in chambers G1 and G3.

Geometric parameters of the HPSA

The geometric parameters of the HPSA are determined based on the technical characteristics of the machines and shown in Fig. 2.

$S_{e1}...S_{e5}$ — extra stroke of the shock absorber elements;

S_{d_comp}, S_{d_reb} — dynamic compression and rebound stroke, respectively;

$S_{full} = S_{d\_comp} + S_{d\_reb}$ — full stroke of the shock absorber;

S_{p2} — stroke of the pneumatic piston at full stroke of the hydraulic piston;

h_{p1} — height of the hydraulic piston;

h_{p2} — height of the pneumatic piston;

d_1, L_1 — diameter and length of the hydraulic cylinder;

d_2, L_2 — diameter and length of the pneumatic cylinder;

δ_{wall} — thickness of the cylinder walls;

δ_g — gap between the cylinders;

L_{max}, L_{min} — maximum and minimum length of the HPSA;

L_{av} — average length of the HPSA, which is comparable with the length at the resultant load P_{des};

L_{br_up}, L_{br_low} — distance from the pneumatic cylinder to the center of the upper and lower mounting bracket, respectively.

Analysis of the elastic response of the HPSA

We investigated the extreme indicators of the suspension resisting dynamic loads during vehicle

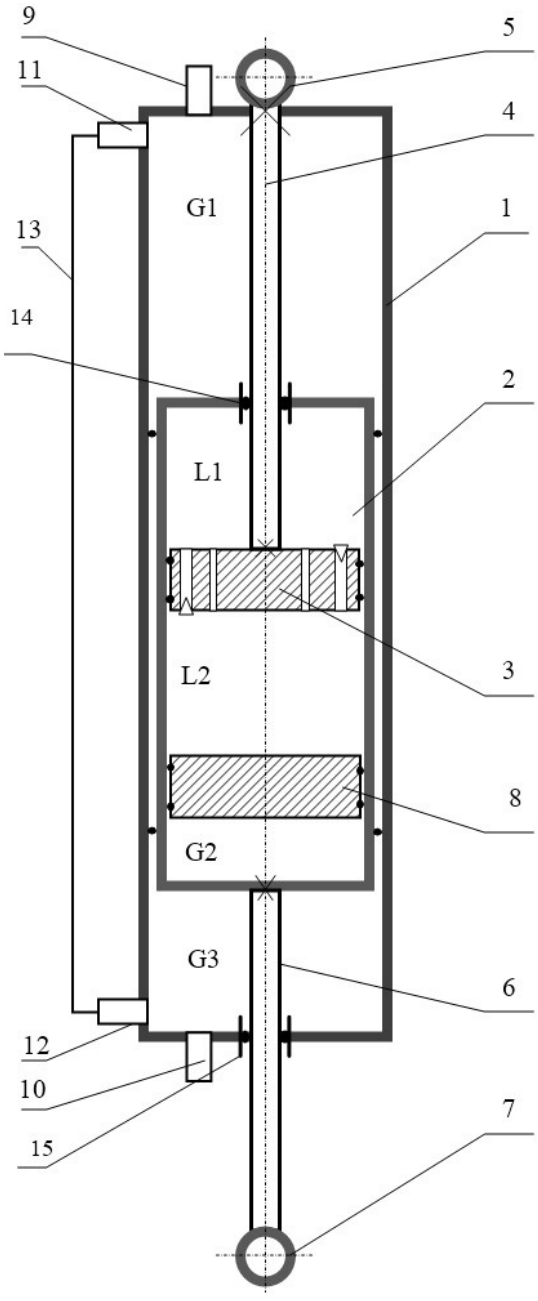

Fig. 1. Shock absorber design: 1 — a pneumohydraulic shock absorber (filled with gas under pressure — chambers G1, G2, G3); 2 — an operating cylinder (filled with liquid); 3 — a hydraulic piston; 4, 6 — a rod; 5, 7 – a rod eye; 8 — a pneumatic piston; 9, 10 — a nipple; 11, 12 — safety valves; 13 — a pipe; 14, 15 — a sealing guide bushing; G1 — an upper gas chamber; G2 — a compensation gas chamber; G3 — a lower gas chamber; L1 — an upper hydraulic chamber; L2 — a lower hydraulic chamber

movement. First of all, we analyzed its indicators determining the elastic component of the suspension and acting on the wheel during movement of the suspension elements (Fig. 3) according to a particular method (Dobromirov et al., 2006; Rotenberg, 1972):

- at curb weight — P_{curb};
- static HPSA deflection — S_{st};
- displacement during compression — S_{d_comp};
- displacement during rebound — S_{d_reb};
- forces P_{d_comp} on the HPSA at S_{d_comp};
- forces P_{d_reb} on the HPSA at S_{d_reb}.

The algorithm for the analysis of the elastic response is as follows:

1. At the selected static deflection S_{st} and load P_{curb} on the shock absorber (with curb weight), gas pressure in chambers G1, G2 and G3 is selected;

2. Calculation of pressure in chambers G1, G2 and G3 during shock absorber stroke from 0 to full stroke $S_{full} = S_{d\_comp} + S_{d\_reb}$.

3. Plotting of the elastic response.

Calculation of gas pressure in chambers G1, G2, G3 at THM curb weight

The shock absorber rod force is determined by the difference in the values of pressure in chambers G1 and G3: p_1 and p_3:

$$P = (p_1 - p_3)F_1,$$

where F_1 — the cross-sectional area of the inner surface of cylinder 1 (Fig. 1).

$$F_1 = (d_1 - d_r)^2 / 4,$$

where d_1 and d_r — the diameter of cylinder 1 and the diameter of the rod, respectively.

Then pressure p_{1curb} in chamber G1 under load at curb weight P_{curb} can be found based on the following relations:

$$\Delta p_{curb} = \frac{P_{curb}}{F_1},\ p_{1curb} = \Delta p_{curb} - p_{3curb}.$$

where p_{3curb} — the selected pressure in chamber G3 under load at curb weight P_{curb}.

Restrictive conditions when selecting pressure:

– the minimum pressure in chamber G3 shall exceed atmospheric pressure;

– the maximum pressure in the gas chambers shall not exceed 4 MPa (Dobromirov, 2006). It is expedient to adopt pressure in chamber G2 to be equal to p_{1curb}.

Changes in pressure during compression

The volume of chamber G1 during compression varies from the average value V_{1av} at the average length L_{av} of the shock absorber, corresponding to static deformation S_{st}, to the minimum value V_{1min} at the length of the shock absorber L_{min}, corresponding to dynamic compression deformation S_{d_comp}:

$$V_{1av} = F_1 \cdot (S_{d\_comp} + S_{e1}),$$

$$V_{1\min} = F_1 \cdot S_{e1}.$$

Then pressure in chamber G1 during dynamic compression will be as follows:

$$p_{1d\_comp} = p_{1curb}\left(\frac{V_{1av}}{V_{1\min}}\right)^n,$$

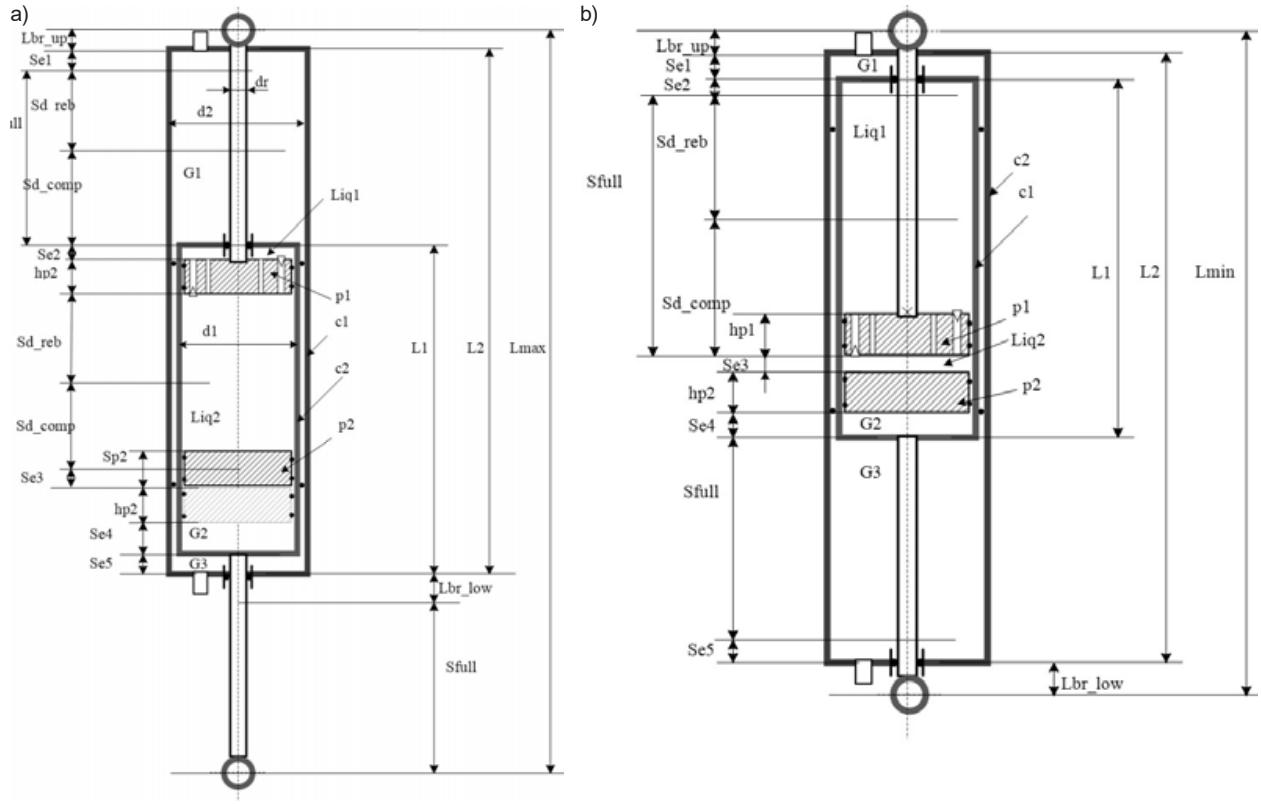

Fig. 2. Design scheme of the geometric parameters at the maximum (a) and minimum (b) length of the shock absorber

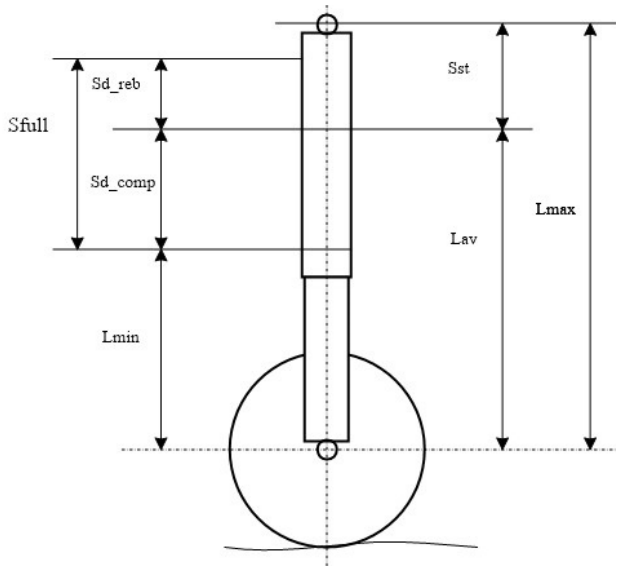

Fig. 3. Shock absorber parameters

where n is the polytropic index (n = 1.26) (Dobromirov et al., 2006; Rotenberg, 1972).

The volume of chamber G3 during compression varies from the average value V_{3av} at the average length L_{av} of the shock absorber, corresponding to static deformation S_{st}, to the maximum value V_{3max} at the length of the shock absorber L_{min}, corresponding to dynamic compression deformation S_{d_comp}:

$$V_{3av} = F_1 \cdot (S_{d\_reb} + S_{e5}),$$

$$V_{3\max} = F_1 \cdot \left(S_{full} + S_5\right).$$

Then pressure in chamber G1 during dynamic compression will be as follows:

$$p_{3d\_comp} = p_{3curb}\left(\frac{V_{3av}}{V_{3\max}}\right)^n.$$

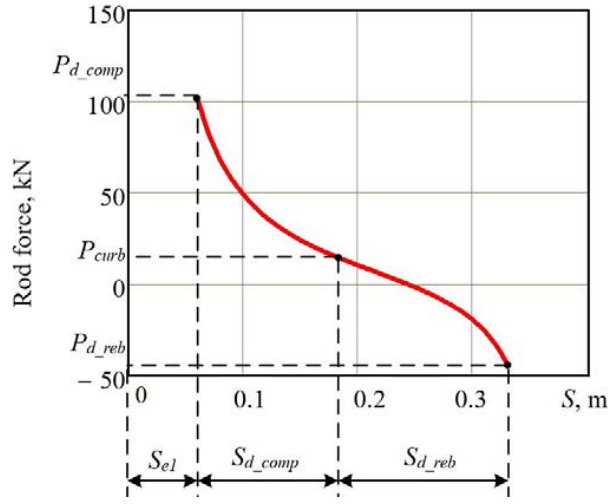

Fig. 4. Results of indicators for the elastic response of the shock absorber in Mathcad

Changes in pressure during rebound

The volume of chamber G1 during rebound varies from the average value V_{1av} at the average length L_{av} of the shock absorber, corresponding to static deformation S_{st}, to the maximum value V_{1max} at the length of the shock absorber L_{max}, corresponding to dynamic rebound deformation S_{d_reb}:

$$V_{1\max} = F_1 \cdot \left(S_{full} + S_{e1}\right).$$

Then pressure in chamber G1 during dynamic rebound will be as follows:

$$p_{1d\_reb} = p_{1curb}\left(\frac{V_{1av}}{V_{1\max}}\right)^n.$$

The volume of chamber G3 during rebound varies from the average value V_{3av} at the average length L_{av} of the shock absorber, corresponding to static deformation S_{st}, to the minimum value V_{3min} at the length of the shock absorber L_{max}, corresponding to dynamic rebound deformation S_{d_reb}:

$$V_{3\min} = F_1 \cdot S_{e5}.$$

Then pressure in chamber G3 during dynamic rebound will be as follows:

$$p_{3d\_reb} = p_{3curb}\left(\frac{V_{3av}}{V_{3\min}}\right)^n.$$

Elastic response in the HSA rod stroke function

The HPSA stroke varies from L_{min} to L_{max} (Fig. 2). In this case, the volumes V_1 and V_3 and pressures p_1 and p_3 in the stroke function S of the rod (S = 0...S_{full}) are as follows:

$$V_1(S) = F_1 \cdot \left(S_{e1} + S\right),\ V_3(S) = F_1 \cdot \left(S_{e5} + S_{full} - S\right),$$

$$p_1(S) = p_{1d\_comp} \cdot \left(\frac{V_1(S_{d\_comp})}{V_1(S)}\right)^n,$$

$$p_3(S) = p_{3d\_comp} \cdot \left(\frac{V_3(S_{d\_comp})}{V_3(S)}\right)^n.$$

Now we can determine the perpendicular load on the wheel from the HPSA deformation:

$$P(S) = F_1 \cdot \left[p_1(S) - p_3(S)\right].$$

Fig. 4 shows a potential model of the relationship under consideration for the KAMAZ-43502 chassis, developed in the Mathcad environment. It should be noted that in some cases S_{d_comp} meet the stated HPSA indicators, and then the load P_{d_reb} is different from the rest, or at least from other, HPSA. The load P_{d_reb} will be negative, which has not been previously observed in the theory of shock absorbers. As a result, a separate group of stated HPSA indicators at the S_{d_reb} graph section bends in the direction opposite to the standard one. The main result is an indication of the fact that the HPSA compression force is directly proportional to the forces acting during HPSA rebound as deformation S_{d_reb} increases. This phenomenon is due to the following: during full rebound, gas is heavily compressed in chamber

G3, and pressure in chamber G1 is minimal (see the equation above).

It is the presented relationship that provides conditions for zero HPSA bottoming during rebound.

Discussion

The modeling in Mathcad shows the probability of a wide range of changes in the characteristics by modifying the initial HPSA configuration: diameter, indicator of auxiliary displacements in chamber G3 vs. the actual forces.

Conclusions

1. The considered design scheme of the shock absorber makes it possible to increase the movement smoothness of THM due to the new scheme for the installation of gas springs, which significantly reduces the probability of HPSA bottoming in all modes of operation.

2. The efficiency of performance of the new HPSA design is confirmed by mathematical modeling in the Mathcad environment.

Acknowledgments

The authors express their gratitude to Viktor Nikolayevich Dobromirov, Professor at the Department of Land Transport and Technological Machines of the Saint Petersburg State University of Architecture and Civil Engineering, for his help and support in developing a new device and writing this paper.

References

Audi (2001). *Pneumatic suspension systems. Part 1. Clearance regulation in Audi A6. Design and operation. Self-training program 242*. [online] Available at: http://rep-air.ru/ssp242.pdf [Date accessed 20.10.2022].

Akopyan, R. A. (1979). *Pneumatic suspension of transport vehicles*. Lvov: Vishcha Shkola, 218 p.

Carway.info (2017). *ALCA®: Ridigity — an issue of measure*. [online] Available at: https://carway.info/ru/content/alcar-zhestkost-vopros-mery [Date accessed 20.10.2022].

Chelomey, V. N. (ed.) (1981). *Vibration in engineering. Reference book in 6 volumes. Vol. 1*. Moscow: Mashinostroyenie, 352 p.

Dobromirov, V. N., Gusev, Ye. N., Karunin, M. A., and Khavkhanov, V. P. (2006). *Shock absorbers. Design. Calculation. Testing.* Moscow: Moscow State Technical University "MAMI", 184 p.

Repin, S. V. (2022). *Pneumohydraulic shock absorber*. Patent RU208894U1.

Repin, S. V., Dobromirov, V. N., Orlov, D. S., and Kapustin, A. A. (2019). The study of the elastic characteristics of the new hydro-pneumatic shock absorber. *Bulletin of Civil Engineers*, No. 5 (76). pp. 260–269. DOI: 10.23968/1999-5571-2019-16-5-260-269.

Repin, S., Bukirov, R., and Vasilieva, P. (2020). Study on effects of damping characteristics of base chassis suspension on operational safety of transport and handling machinery. *Transportation Research Procedia*, Vol. 50, pp. 574–581. DOI: 10.1016/j.trpro.2020.10.069.

Rotenberg, R. V. (1972). *Motor vehicle suspension. Vibrations and running smoothness. 3rd edition*. Moscow: Mashinostroyenie, 392 p.

Techautoport.ru (2022). *Design and operation of pneumatic suspension*. [online] Available at: https://techautoport.ru/hodovaya-chast/podveska/pnevmaticheskaya-podveska.html [Date accessed 20.10.2022].

Zaitsev, A. V. (2007). *Calculation of vehicle suspension parameters*. Kurgan: Kurgan State University, 16 p.

Zhileykin, M. M., Kotiev, G. O., and Sarach, Ye. B. (2012). Method for calculating characteristics of pneumatic-hydraulic controlled suspension with two-level damping in multi-axle vehicles. *Science & Education*, No. 1, 77-30569/346660. [online] Available at: http://technomag.edu.ru/doc/346660.html. [Date accessed 20.10.2022].

Lukin, P. P., Gasparyants, G. A., and Rodionov, V. F. (1984). *Design and analysis of vehicles*. Moscow: Mashinostroyenie, 376 p.

ИССЛЕДОВАНИЕ РАБОТЫ БЕСПРОБОЙНОГО ПНЕВМОГИДРАВЛИЧЕСКОГО АМОРТИЗАТОРА В ПОДВЕСКЕ ТРАНСПОРТНО-ТЕХНОЛОГИЧЕСКОЙ МАШИНЫ

Сергей Васильевич Репин*, Иван Иванович Воронцов, Денис Сергеевич Орлов,
Роман Андреевич Литвин

Санкт-Петербургский государственный архитектурно-строительный университет
Санкт-Петербург, Россия

*E-mail: repinserge@mail.ru

Аннотация
Введение: Плавность хода транспортно-технологических машин (ТТМ) (экскаваторов, кранов, оборудования для содержания дорог и т.п.) на автомобильном шасси значительно сказывается на их долговечности в силу большой массы оборудования и неравномерности распределения нагрузок по осям базового шасси, что вызывает большие динамические нагрузки при перемещении по дорогам с несовершенным покрытием. Зачастую, именно по таким дорогам приходится перемещаться ТТМ. **Цель исследования:** повышение плавности хода ТТМ на автомобильном шасси на основе использования новой конструкции амортизатора, как главного элемента подвески ходовой части машины. **Методы:** Конструкция амортизатора с гидропневматической схемой считается более распространенной. Принцип их работы основан на гидравлическом сопротивлении, возникающем при движении поршня со штоком в объем заполненном маслом, при этом газ в закрытой части уплотняется, компенсируя изменения внутреннего объема. Главным отрицательным показателем гидропневматического амортизатора (ГПА) чаще всего бывает вероятность пробоя при эксплуатации в момент наезда на барьер (препятствие), что влечет за собой динамические нагрузки, уменьшающие ресурс машины и деталей самого амортизатора. **Результаты:** В статье описывается новая конструкция амортизатора, исключающего пробой, приводится математическая модель его упругой характеристики и результаты моделирования в Mathcad, подтверждающие работоспособность устройства.

Ключевые слова: плавность хода, амортизатор, упругая характеристика.